TRANSIT TIMING OBSERVATIONS FROM *KEPLER*. VIII CATALOG OF TRANSIT TIMING MEASUREMENTS OF THE FIRST TWELVE QUARTERS

Tsevi Mazeh[1], Gil Nachmani[1], Tomer Holczer[1], Daniel C. Fabrycky[2], Eric B. Ford[3], Roberto Sanchis-Ojeda[4], Gil Sokol[1], Jason F. Rowe[5], Eric Agol[6], Joshua A. Carter[7], Jack J. Lissauer[5], Elisa V. Quintana[8], Darin Ragozzine[3], Jason H. Steffen[9], William Welsh[10]

Received _____; accepted _____

[1] School of Physics and Astronomy, Raymond and Beverly Sackler Faculty of Exact Sciences, Tel Aviv University, Tel Aviv 69978, Israel

[2]Department of Astronomy and Astrophysics, University of Chicago, 5640 Ellis Ave., Chicago, IL 60637, USA

[3]Astronomy Department, University of Florida, Gainesville, FL 32111, USA

[4]Department of Physics, and Kavli Institute for Astrophysics and Space Research, Massachusetts Institute of Technology, Cambridge, MA 02139, USA

[5]NASA Ames Research Center, Moffett Field, CA 94035, USA

[6]Department of Astronomy, Box 351580, University of Washington, Seattle, WA 98195, USA

[7]Hubble Fellow, Harvard-Smithsonian Center for Astrophysics, 60 Garden Street, Cambridge, MA 02138, USA

[8]SETI Institute, 189 Bernardo Ave, Suite 100, Mountain View, CA 94043, USA

[9]Fermilab Center for Particle Astrophysics, P.O. Box 500, MS 127, Batavia, IL 60510, USA

[10]Astronomy Department, San Diego State University, 5500 Campanile Drive, San Diego, California 92182, USA

ABSTRACT

Following Ford et al. (2011, 2012) and Steffen et al. (2012a) we derived transit timing variations (TTVs) of the *Kepler* KOIs, using the first twelve quarters of the *Kepler* data. Simultaneously with its timing, we obtained for each transit its duration and depth, presenting the results as a catalog for the community to use. We derived a few statistics of our TTVs that could be used to indicate significant variations. Including systems found by previous works, we pointed out 100 KOIs that showed highly significant TTV, 9 of which had short-period TTV modulations with small amplitudes. We considered two effects that could cause *apparent* periodic TTV — the finite sampling of the observations and the interference with the stellar activity, stellar spots in particular. We briefly discuss some statistical aspects of our detected TTVs. We show that the TTV period is correlated with the orbital period of the planet and the TTV amplitude.

Subject headings: planetary systems – planets and satellites: detection – techniques: miscellaneous

1. Introduction

Since 2009 May 2, the *Kepler* spacecraft has been collecting science-quality photometric data of more than 150,000 stars. Based on the first 5 months of data, Borucki et al. (2011, hereafter B11) identified 1235 planet candidates associated with 997 host stars. Analysis of the first 16 months of data (Batalha et al. 2012, hereafter B12) yielded an additional 1091 viable planet candidates — termed as Kepler objects of interest, or KOIs. The almost uninterrupted accurate *Kepler* light curves of these KOIs enable the community to detect minute changes in the observed transit light curves. This is especially true for the individual times of transit, which for some KOIs show variation (=TTV) relative to a linear ephemeris that assumes a constant Keplerian orbit. These TTVs can indicate a dynamical interaction with additional objects in the system, as was predicted by the seminal works of Holman & Murray (2005) and Agol et al. (2005). Indeed, TTVs turn out to be a crucial tool in the study of systems with known multiple transiting planets (e.g., Holman et al. 2010; Lissauer et al. 2011a; Cochran et al. 2011; Fabrycky et al. 2012; Steffen et al. 2012b).

However, TTVs can do much more. They may indicate dynamical interactions with unseen, otherwise undetected, additional objects in the system (e.g., Ballard et al. 2011). Therefore, it can be useful to perform a systematic search of all KOIs, as was done in the work of Ford et al. (2011, hereafter F11) and was continued with Ford et al. (2012, hereafter F12) and Steffen et al. (2012a, hereafter S12) work based on the first six quarters of Kepler data. This paper is a follow-up of F11, F12 and S12 studies (see also the catalog of Rowe et al., private communication), presenting a systematic analysis of the first *twelve* quarters of the *Kepler* data of all KOIs. The goal is to produce an easy-to-use catalog that can stimulate further analysis of interesting systems and statistical analysis of the Kepler KOIs with significant TTV as a sample.

After presenting the details of our pipeline and the catalog itself (Section 2), we derive

a few statistical characteristics of each TTV series that can identify the ones with significant variations (Section 3). Sections 4 & 5 list 100 systems with highly significant TTVs, and Section 6 comments on some interesting systems, in particular the ones for which the derived TTVs could be of non-physical origin. In Section 7 we present a few basic statistical features of the sample of the 100 systems, and briefly discuss the possible use of the catalog.

2. Analysis of the transit light curves

The Kepler long-cadence data were downloaded from the archive.stsci.edu ftp server (ftp://archive.stsci.edu/pub/kepler/lightcurves/tarfiles). We obtained data for 2318 KOIs, listed in B11 and/or B12 ($http://archive.stsci.edu/kepler/planet\_candidates.html$). We did not analyze 188 KOIs:

- 51 KOIs of $SNR < 10$, which we opted not to analyze.
- 21 KOIs did not have enough information for our pipeline. 20 KOIs had only one transit and one KOI did not have a measured transit duration.
- 116 KOIs had very short transit duration of less than 1.5 hours, which resulted in less than 3 points per transit.

Out of the remaining 2130 KOIs, our program did not succeed in analyzing 7 KOIs: 5 KOIs produced a bad model and 2 had very long orbital periods resulting in only 2–3 measurements, which left us with 2123 KOIs that are included in Tables 1 & 2. However, 86 KOIs had less than 7 acceptable TTV measurements, and therefore we did not include them in the statistical analysis. We were left with 2037 KOIs (see Table 3).

We started by folding the *Kepler* light curve of each KOI with the ephemeris of B11 and/or B12, in order to obtain the best possible template for the transit light curve (see

F11 for details). In order to reserve some flexibility for the fitted model we opted not to use the Mandel & Agol (2002) model, which used a specific transit shape with a given limb-darkening function, ignoring, for example, any stellar gravity darkening. We used instead an analytical function that could mimic different transit shapes. In particular, we allowed a slight asymmetry in our model, based on the example of KOI-13 (Szabó et al. 2011, see also Mazeh et al. 2012). Such a flexibility came with a price. When the folded light curve of a transit had a low SNR, the algorithm adopted a strange shape which was obviously wrong. For such cases we added an option to fit the data with a second model, which is less flexible but maintained a realistic transit profile.

We used the best-fit transit model as a template to measure the actual timing of each individual transit (=TT) and derive its TTV — the difference between the TT and the expected time, based on the linear ephemeris. The TT derivation was performed while allowing the duration — TDV, and depth — TPV, of each transit to vary as well. As our template was just a mathematical function, the TTV, TDV and TPV were equivalent to moving the center of the template or stretching it in the time and flux dimensions. In our approach, we searched for the minimum of the sum-of-squared residuals, the standard χ^2 function, in the three parameter space.

Although the main emphasis of this paper was the TTVs of the KOIs, we opted to vary the three parameters of the template simultaneously, as we found a few KOIs for which the transit duration or depth did vary significantly, either because of physical processes, or as a results of some observational effects. One example is, again, KOI-13, for which Szabó et al. (2012a) have found some indications for a long-term variation of the impact parameter, which is equivalent to the variation of the transit duration. Our analysis, based now on twelve quarters, confirmed Szabó et al. (2012a) results and are presented in Figure 1. One can see in that figure the highly significant linear duration variation of KOI-13, which

amounts to $\sim 1\%$ peak-to-peak modulation over the entire span of the data. For such cases the simultaneous analysis of TTV, TDV, TPV was an advantage, and, in principle, could yield better TTVs.

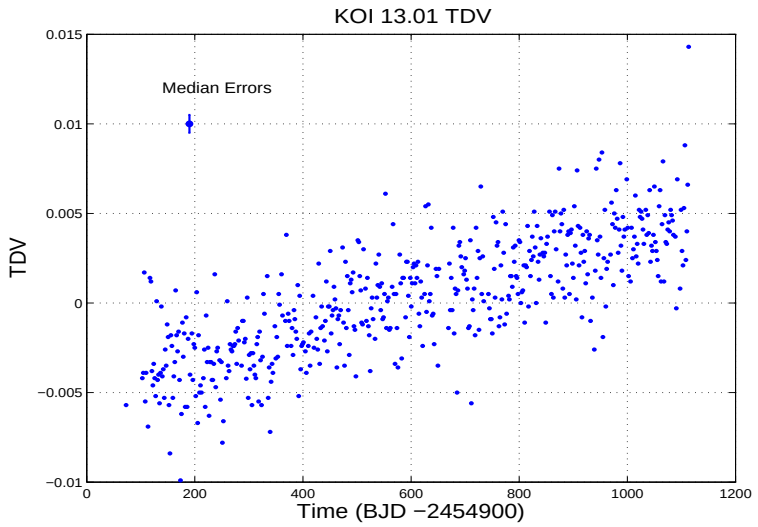

Fig. 1.— The TDV (duration variation) of KOI-13.01. Each point represents our best estimate for the deviation of the transit duration from its averaged value.

However, for low-SNR transits the three-parameter simultaneous minimization of the χ^2 function could give completely erroneous results, based on some local minimum in a noisy χ^2 surface. We therefore had to strictly vet our results and reject any suspicious findings. As a result we did not report in our catalog TTV, TDV or TPV for some transits. We believe that many of those transits would yield suspicious TTVs anyway, and therefore the price we paid for the simultaneous fitting was not too high.

2.1. The model for a transit

We select our best model for the folded transit among two templates — a Legendre-based and a Fermi-based model. Both models assume that the light curve has a unity

value outside the transit, which lasts from t_1 until t_4. The choice between the two is made according to their goodness of fit, i.e. the model with the lower χ^2. We further make sure that the model has one local minimum only.

The Legendre-based model has the form:

$$F(\tau) = \sum_{k=1}^{N} \left[A_k L^k(\tau) + S_k sin(\pi k/2 \cdot \tau) + C_k cos(\pi k/2 \cdot \tau) \right], \quad (1)$$

where L^k is the Legendre polynomial of order k, τ is the normalized phase of the transit, such that at the beginning of the ingress $\tau(t_1) = -1$, and at the end of the egress $\tau(t_4) = +1$, A_k, S_k and C_k are linear parameters found through a linear optimization model, and $N = 10$ is the maximum order we allowed. We optimize the model through varying the phases of t_1 and t_4 within the orbital period. We avoid local bumps in the model by reducing its order and by using local linear fits when needed.

The Fermi-based model has the form:

$$F(\tau) = 1 + M \left[\frac{1}{e^{(\tau+\varphi+\mu)/s} + 1} + \frac{1}{e^{(\tau+\varphi-\mu)/s} + 1} - 1 \right], \quad (2)$$

where τ is the phase of the transit, as for the Legendre model, and φ, s, μ and M are free parameters which define the phase shift, steepness, width and depth of the transit. In order to obtain a more "transit-like" shape, the points between the ingress and egress are replaced by a parabola, with its width as another free parameter, under the analytical constraint that the resulting function and its first derivative are both continuous. We used Markov chain Monte Carlo (MCMC) process to find the best values of the five parameters.

In most KOIs the selected function was the Legendre-based model, while the Fermi-based one was typically selected only when the SNR of the folded light curve was low.

2.2. Finding the best TTV, TDV and TPV

The derivation of the TTV, TDV and TPV was done after we fitted a polynomial to the light curve on the two sides of each transit, in order to remove the stellar and instrumental long-term photometric variations at the time of each transit. We minimized the standard χ^2 function, assuming each cadence has the same error. The errors on each TTV, TDV and TPV were estimated by searching for the first point for which $\Delta\chi^2 = 1$ relative to its minimum value. The scatter around the polynomial fit before and after each transit was used as our best estimate for the error of the individual *Kepler* measurements at that transit.

For each KOI, we rejected outlier TTVs, either because the TTV value was too different from the other TTVs of this KOI, or because the TTV error estimate was too large. Usually a large error meant that some photometric measurements during that transit were erroneous. Like in Ford et al. (2011), we iterated the procedure, aligning the transits based on the measured TTVs, in order to generate a better transit model, and then recomputed the TTV, TDP and TPV.

Table 1 lists the modified ephemerides of the KOIs, based on our analysis, and the duration and depth of their transit, derived from the folded light curve. The transit duration is given as a fraction of the orbital period and the depth is given in units of the stellar intensity outside the transit. Table 2 lists our derived TTV, TDV and TPVs for 170438 transits. We list the transit number, its expected time, and then its TTV/TDV/TPV with their uncertainties, respectively. The TDV and the TPV are given in units of the transit duration and depth.

Table 1: Linear ephemerides of the KOI transits, together with their durations and depths

KOI	T_0[a] [d]	Period [d]	Duration[b]	Depth[c]
1.01	55.762503	2.47061339	0.0369	0.01412
	±0.000008	±0.00000003		
2.01	54.357917	2.20473527	0.0837	0.00667
	±0.000018	±0.00000006		
3.01	57.812653	4.88780170	0.0242	0.00433
	±0.000033	±0.00000027		
4.01	90.526022	3.84937091	0.0334	0.00131
	±0.000311	±0.00000188		
5.01	65.973225	4.78032754	0.0215	0.00096
	±0.000232	±0.00000179		
7.01	56.611798	3.21366637	0.0615	0.00073
	±0.000369	±0.00000203		
10.01	54.118496	3.52249844	0.0425	0.00913
	±0.000055	±0.00000031		
12.01	79.596487	17.85521360	0.0208	0.00901
	±0.000344	±0.00000992		
13.01	53.565129	1.76358761	0.0858	0.00457
	±0.000009	±0.00000003		
17.01	54.485703	3.23469926	0.0514	0.01057
	±0.000032	±0.00000018		

[a] BJD-2454900.

[b] In units of the orbital period

[c] In units of the stellar intensity outside the transit

(This table will be available in its entirety in a machine-readable form. A portion is shown here for guidance regarding its form and content.)

Table 2: TTV, TDV and TPV of the *Kepler* KOIs

n	t_n[a] [d]	TTV_n [min]	σ_n [min]	TDV_n	σ_n	TPV_n	σ_n
0	55.7625	−0.034	0.096	0.0055	0.0027	−0.0116	0.0026
1	58.2331	0.06	0.077	0.0025	0.0021	−0.0129	0.0021
2	60.7037	−0.13	0.1	0.0045	0.0026	−0.0149	0.0028
3	63.1743	−0.03	0.13	0.0018	0.0032	−0.016	0.0034
4	65.645	−0.21	0.11	0.0015	0.0026	−0.0032	0.0029
5	68.1156	−0.021	0.087	−0.0007	0.0022	−0.0046	0.0024
6	70.5862	0.06	0.1	−0.0016	0.0027	−0.0088	0.0028
7	73.0568	0.13	0.11	0.018	0.0032	−0.0333	0.003
8	75.5274	0.17	0.11	0.0043	0.0034	−0.0045	0.0032
9	77.998	0.04	0.11	−0.0056	0.0035	0.0027	0.0032

[a] BJD-2454900.

(This table will be available in its entirety in a machine-readable form. A portion of the table of KOI-1.01 is shown here for guidance regarding its form and content.)

3. Identification of KOIs with significant TTV

As the main interest of this study is the TTVs of the KOIs, the next sections concentrate on the analysis of the derived TTV. Analyses of TDVs and TPVs are deferred to a later paper.

In order to identify KOIs with significant TTVs, we compute a few statistics (see F11, F12 and S12) that characterize some modes of the scatter of the derived TTVs, all presented in Table 3.

- For each KOI, we compare the MAD_{TTV} — the median absolute deviation of the TTVs, which is a measure of their scatter, and σ_{TTV}, their median error (see F11 for details). High values of MAD_{TTV}, relative to σ_{TTV}, may indicate significant TTV, especially because the MAD statistic is not so sensitive to outliers. However, the derived ratio relies on our estimate of the TTV error, which by itself depends on the estimated error and the nature of the noise of the *Kepler* measurements. As we are not sure what contribution red noise makes to the total noise of the *Kepler* measurements, we do not rely on our estimate of the TTV error, and therefore do not use the MAD to σ ratio to identify KOIs with significant TTVs. The two values are given in the table for completeness.

Another drawback of the MAD to σ ratio is its insensitivity to the order of the residuals. That is, any permutation of the residuals yields the same two values. However, as pointed out by F11 (see also Agol et al. 2005; Holman & Murray 2005), the expected timescale of the dynamical interaction between planets is in most cases larger than the orbital period of the transiting planet, and therefore we expect long-term correlation in the planet's TTVs, if indeed the planet is subject to a dynamical perturbation.

We therefore add three statistics that can indicate long-term correlation of the TTVs.

- The Lomb-Scargle (LS) periodogram (e.g., S12), which searches for a cosine-shape periodicity in the series of TTVs. We identify the highest peak in the periodogram and assign a false-alarm probability (FAP) to the existence of the associated periodicity in the data. This is done by calculating similar 10^4 LS periodograms with different random permutations of the same TTVs, and obtaining the highest peak in each of these periodograms. The best period and log of its p-value are listed in Table 3.

- A long-term polynomial fit to the series of TTVs. A good polynomial fit usually indicates a long-term modulation with a time scale longer than the data span. We search for a polynomial with degree lower than 4, choose the best fit and check its significance with the $\mathcal{F}$ test (e.g., F11). The log of the p-value of the best polynomial fit is also given in Table 3.

- The alarm score $\mathcal{A}$ of Tamuz, Mazeh & North (2006), which is sensitive to correlation between adjacent TTVs. The value of $\mathcal{A}$ reflects the number of consecutive TTVs with the same sign, without assuming any functional shape of the modulation (see Tamuz, Mazeh & North (2006) for a detailed discussion). This is done relative to a constant, zero TTV assumption. We assign a false-alarm probability to the occurrence of the obtained score by calculating alarm scores for 10^4 different random permutations of the same TTVs. The alarm score and the log of its p-value are listed in Table 3.

Table 3 can be used to identify KOIs with significant TTVs of various timescales.

4. KOIs with significant TTVs

In this section we point out 91 systems with highly significant TTVs, plotted in Figures 2–13, and summarized in Table 4. Seventy six of those KOIs show some periodicity,

Table 3: Statistical parameters for TTVs of Kepler KOIs

KOI	σ [min]	MAD [min]	LS Period [d]	LS Peak	p-LS [log]	$\mathcal{A}$	p-$\mathcal{A}$ [log]	Pol. Deg.	p-$\mathcal{F}$ [log]
1.01	0.0853	0.0628	10.8	5.43	−0.1	−0.033	−0.5	2	−0.3
2.01	0.2392	0.1556	5.36	6.05	−0.1	0.233	−1.2	2	−0.3
3.01	0.1735	0.1802	34.8	5.42	−0.2	−0.499	−0.1	2	−0.3
4.01	2.2182	2.031	10.41	6.2	−0.4	−0.419	−0.1	2	−0.3
5.01	1.6114	1.0833	14.64	6.62	−0.6	−0.183	−0.3	1	−0.3
7.01	3.3156	2.2459	45.48	5.59	−0.1	−0.066	−0.5	1	−0.3
10.01	0.5838	0.4043	75.82	5.36	−0.1	−0.2	−0.1	2	−0.3
12.01	0.6881	0.9077	1061.48	7.64	−2	0.873	−1.6	2	−0.4
13.01	0.1689	0.0921	5.72	6.18	−0.1	−0.244	−0.1	3	−0.3
17.01	0.3259	0.2713	10.7	9.04	−1.4	−0.102	−0.3	2	−0.3

(This table will be available in its entirety in a machine-readable form. A portion is shown here for guidance regarding its form and content.)

with time scales ranging from $\sim$ 200 to $\sim$ 1400 days and amplitudes in range of $\sim$ 10 to $\sim$ 1200 min. For each of the 76 systems, we suggest a possible continuous fit to the TTVs, composed of a straight line, which can present a correction to the orbital period of the transiting planet, *together* with a cosine function with the best-found period. For 47 KOIs, the period, its error and amplitude are given in the table. For 28 systems the period found was too long and we can not derive its uncertainty. In those cases, the period given is just an approximation. In one special case — KOI-142.01, we fit a straight line with *two* different cosine functions.

For 11 KOIs, the TTV series do not include a maximum *and* a minimum, and therefore a cosine function can not be fitted, probably because the time scale of the modulation is longer than the time span of the data. In those cases, we fit the TTV with a long-term parabola only, and a note is written in the plot and in Table 4. For four systems — KOI-1241.01, 1285.01, 1452.01 and 1546.01, neither a cosine function nor a parabola could be fitted, but the TTVs look nevertheless significant (see Section 6 for s short discussion).

Table 4 lists the KOI number, the orbital period of the transiting planet and the model we use, either a Cosine function, "C", or a polynomial "P". For a Cosine fit, the TTV period and its error, when available, and amplitude are given too. Also listed are the number of TTV measurements, the number of KOIs in this system and references to previous studies, when available. The table includes references to Section 6, where we briefly comment on some of these systems.

Table 4: KOIs with significant TTV

KOI	Period [d]	Model	Period [d]	σ_P [d]	Amp [min]	σ_A [min]	N	Multi-plicity	Ref.
42.01	17.83	C	990	···	13.95	0.86	51	1	
84.01	9.29	C	309	31	4.47	0.41	101	1	[3] Kepler19b
103.01	14.91	C	261.7	8.1	25.64	0.83	62	1	[1,2]
137.01	7.64	C	262	22	4.31	0.41	92	3	[1,4] Kepler18c
137.02	14.86	C	266	25	3.93	0.38	53	3	[1,2,4] Kepler18d
*142.01	10.95	C	632	38	669	15	88	1	[1,2]
			349	19	109	3			
148.01	4.78	C	404	68	4.18	1	144	3	[5] Kepler48b
148.02	9.67	C	411	64	3.46	0.8	74	3	[5] Kepler48c
152.02	27.40	C	640	320	17.6	3.3	24	3	[13]
157.04	46.69	C	590	130	24.9	4.7	18	6	[2,6] Kepler11f
168.01	10.74	C	491	78	22.2	3.6	69	3	[2,7] Kepler23c
*190.01	12.26	C	271	18	4.14	0.33	65	1	[16]
227.01	17.70	C	1600	···	1042.3	6.9	44	1	[1,2]
244.01	12.72	C	362	45	1.04	0.25	63	2	[1,8] Kepler25c
244.02	6.24	C	349	51	3.98	0.43	127	2	[1,2,8] Kepler25b
248.01	7.20	C	368	43	8.87	1	108	4	[1,2,5] Kepler49b
248.02	10.91	C	354	47	16.9	1.9	66	4	[1,5] Kepler49c
250.01	12.28	C	690	260	10.1	1.1	69	4	[8] Kepler26b
250.02	17.25	C	650	···	8.1	1.7	45	4	[1,8] Kepler26c
262.01	7.81	C	740	···	25.2	3.1	108	2	[5] Kepler50b
262.02	9.38	C	860	···	16.1	2.5	87	2	[5] Kepler50c
270.01	12.58	C	193.2	10	16.7	5.2	64	2	[1]
271.02	29.39	C	820	···	13.2	2.4	22	2	
277.01	16.23	C	448	21	119.7	3.3	55	1	[1,2,9] Kepler36c

Table 4: - continued

KOI	Period [d]	Model	Period [d]	σ_P [d]	Amp [min]	σ_A [min]	N	Multi-plicity	Ref.
308.01	35.60	C	640	79	33.3	2.3	27	1	[2]
314.02	23.09	C	1200	···	24.5	2.5	36	3	
315.01	35.59	P	···	···	···	···	25	1	
318.01	38.58	C	590	···	4.57	0.85	19	1	
319.01	46.15	C	305	18	11.7	1.4	20	1	
*341.01	14.34	C	182	11	16.1	2.7	40	2	
345.01	29.88	C	820	···	11.2	1.9	22	1	
350.01	12.99	P	···	···	···	···	55	1	
377.01	19.27	C	980	200	309.9	3.2	38	3	[2,10] Kepler9b
377.02	38.85	C	1010	180	738.4	6.5	18	3	[1,2] Kepler9c
392.01	33.42	C	1200	···	67	33	23	2	
410.01	7.22	P	···	···	···	···	129	1	
448.02	43.59	P	···	···	···	···	19	2	[2]
456.01	13.70	C	720	···	18.8	1.7	60	2	[2]
473.01	12.71	C	820	···	30.9	2.3	60	1	[2]
524.01	4.59	C	331	37	17.5	1.1	196	1	[2]
525.01	11.53	P	···	···	···	···	83	1	
*609.01	4.40	P	···	···	···	···	208	1	[16]
638.01	23.64	P	···	···	···	···	23	2	
738.01	10.34	C	1600	···	70	11	52	2	[2,11] Kepler29b
759.01	32.63	C	1600	···	73	9.6	22	1	
760.01	4.96	P	···	···	···	···	190	1	
775.01	16.38	C	212	21	15.9	3.5	40	3	[5] Kepler52c
775.02	7.88	C	208	14	14.6	2	75	3	[5] Kepler52b

Table 4: - continued

KOI	Period [d]	Model	Period [d]	σ_P [d]	Amp [min]	σ_A [min]	N	Multi-plicity	Ref.
775.03	36.45	C	305	25	11.6	3.6	15	3	
784.01	19.27	C	550	110	14.8	4	40	2	[2]
806.02	60.32	C	730	290	21.2	1.6	12	3	[11,14] Kepler30c
829.01	18.65	C	590	150	16.8	3.5	48	3	[5] Kepler53b
829.03	38.56	C	474	74	25	4.7	23	3	[5] Kepler53c
841.01	15.34	C	760	···	14.2	2.3	51	2	[2,8] Kepler27b
854.01	56.06	C	391	42	9.7	4.1	16	1	[2]
872.01	33.60	C	193	6.9	48.3	5.1	22	2	[2,12] Kepler46b
880.01	26.44	C	940	···	21.4	3.6	29	4	
884.02	20.49	C	805	55	178.6	3.5	36	3	[1,5]
886.01	8.01	C	1200	···	99.6	6.5	78	3	[2,5] Kepler54b
886.02	12.07	C	740	···	23.2	6.9	36	3	[5] Kepler54c
902.01	83.92	P	···	···	···	···	13	1	
904.01	2.21	C	256	34	4	1.5	196	5	
904.02	27.95	P	···	···	···	···	16	5	[5] Kepler55b
904.03	42.15	C	800	···	73	11	10	5	[5] Kepler55c
904.04	4.62	C	196	12	7.6	2.6	97	5	
904.05	10.20	C	116.9	3.7	6.7	2.8	58	5	
918.01	39.64	C	1300	···	14.6	1.6	23	1	[2]
*935.01	20.86	C	880	···	19.5	1.5	38	4	[1,11] Kepler31b
*984.01	4.29	C	487	36	46.4	1.2	62	1	[2]
989.03	16.16	C	1000	···	47.8	8.4	36	1	
1081.01	9.96	C	1100	···	89.9	7.8	85	1	[2]
1102.01	12.33	C	421	50	36.7	5	69	2	[2,7] Kepler24c

Table 4: - continued

KOI	Period [d]	Model	Period [d]	σ_P [d]	Amp [min]	σ_A [min]	N	Multi-plicity	Ref.
1102.02	8.15	C	416	70	24	5	93	2	[2,7] Kepler24b
1145.01	30.59	C	1600	···	304	14	30	1	[2]
1236.01	35.74	C	760	130	68	11	20	2	
*1241.01	21.41	···	···	···	···	···	37	2	[5] Kepler56c
1241.02	10.50	C	547	100	124	24	56	2	[1,5] Kepler56b
1270.02	11.61	C	455	51	26.3	3	43	2	[2,5] Kepler57c
*1285.01	0.94	···	···	···	···	···	778	1	[2,15]
*1452.01	1.15	···	···	···	···	···	767	1	[15]
1529.01	17.98	C	470	110	31.2	7.6	26	2	[2,5] Kepler59c
*1546.01	0.92	···	···	···	···	···	675	1	[15]
1573.01	24.81	C	1500	···	77.2	3.8	28	1	[2]
1581.01	29.54	C	730	···	58	14	29	1	[2]
1599.01	20.42	C	770	···	94	19	19	1	[2]
1802.01	5.25	C	240	20	7.85	0.64	183	1	
1840.01	7.04	C	1500	···	67.4	5	125	1	[2]
1856.01	46.30	C	790	···	39.5	4	21	1	

Table 4: - continued

KOI	Period [d]	Model	Period [d]	σ_P [d]	Amp [min]	σ_A [min]	N	Multi-plicity	Ref.
1884.01	23.11	P	···	···	···	···	21	2	
1907.01	11.35	C	620	···	10.1	1.6	72	1	
2038.01	8.31	C	980	···	37.3	5.1	78	4	

[1]F11

[2]F12

[3]Ballard et al. (2011)

[4]Cochran et al. (2011)

[5]Steffen et al. (2013)

[6]Lissauer et al. (2011a)

[7]Ford et al. (2012)

[8]Steffen et al. (2012b)

[9]Carter et al. (2012)

[10]Holman et al. (2010)

[11]Fabrycky et al. (2012)

[12]Nesvorny et al. (2012)

[13]Wang et al. (2012)

[14]Tingley et al. (2011)

[15]Szabó et al. (2012b)

[16]Santerne et al. (2012)

*Discussed in Section 6

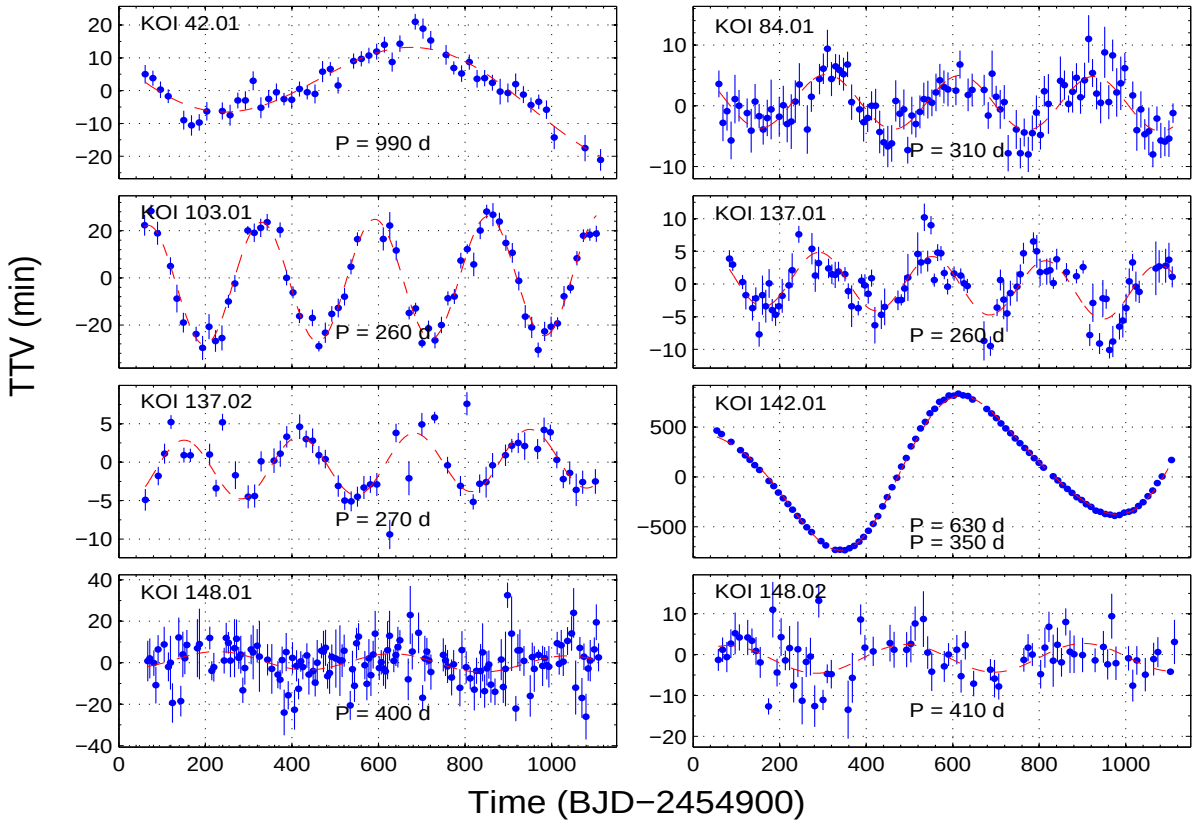

Fig. 2.— KOIs with significant TTVs. The fit, plotted with a dashed line, is composed of a straight line *together* with a cosine function with the best found period. In one case — KOI-142.01, we fitted a straight line with *two* different cosine functions. When the periodicity could not be constrained, like in KOI-448.02, we fitted the data with a parabola only. In such cases, a note is written in the plot.

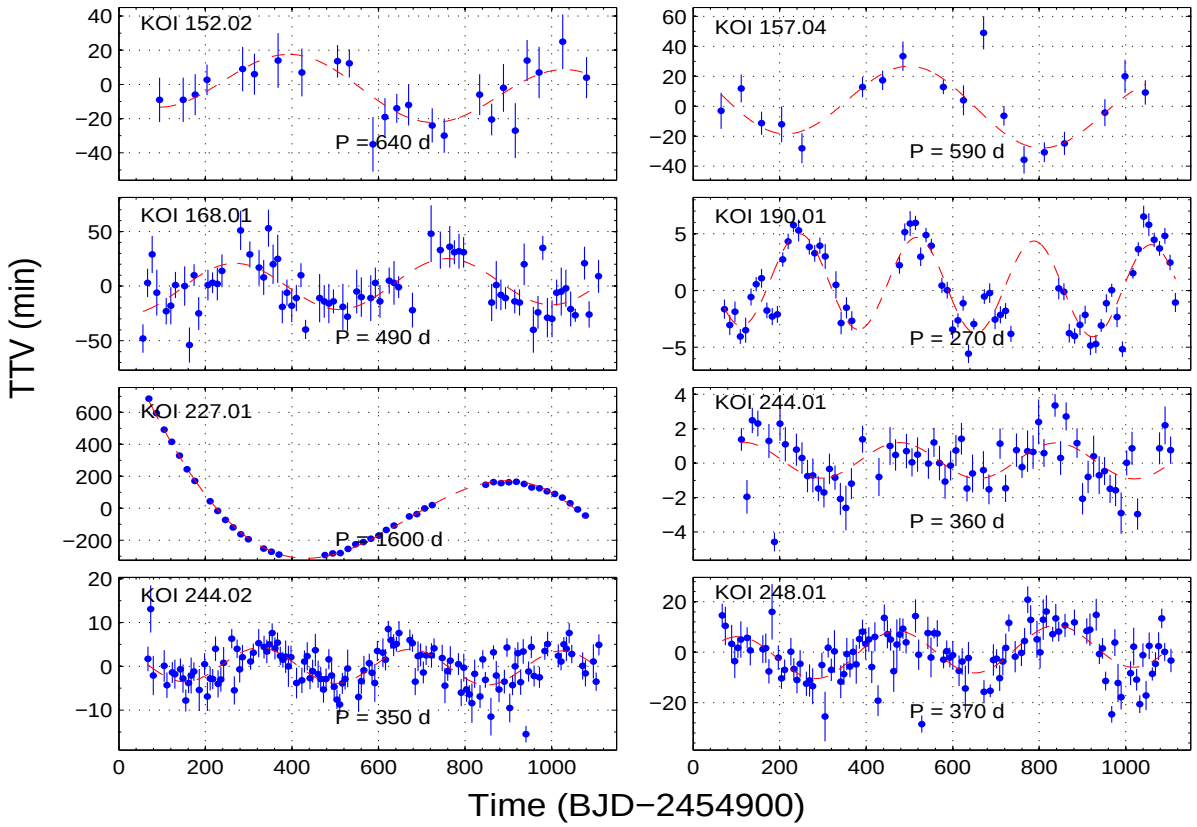

Fig. 3.— KOIs with significant TTVs. See Figure 2 for details.

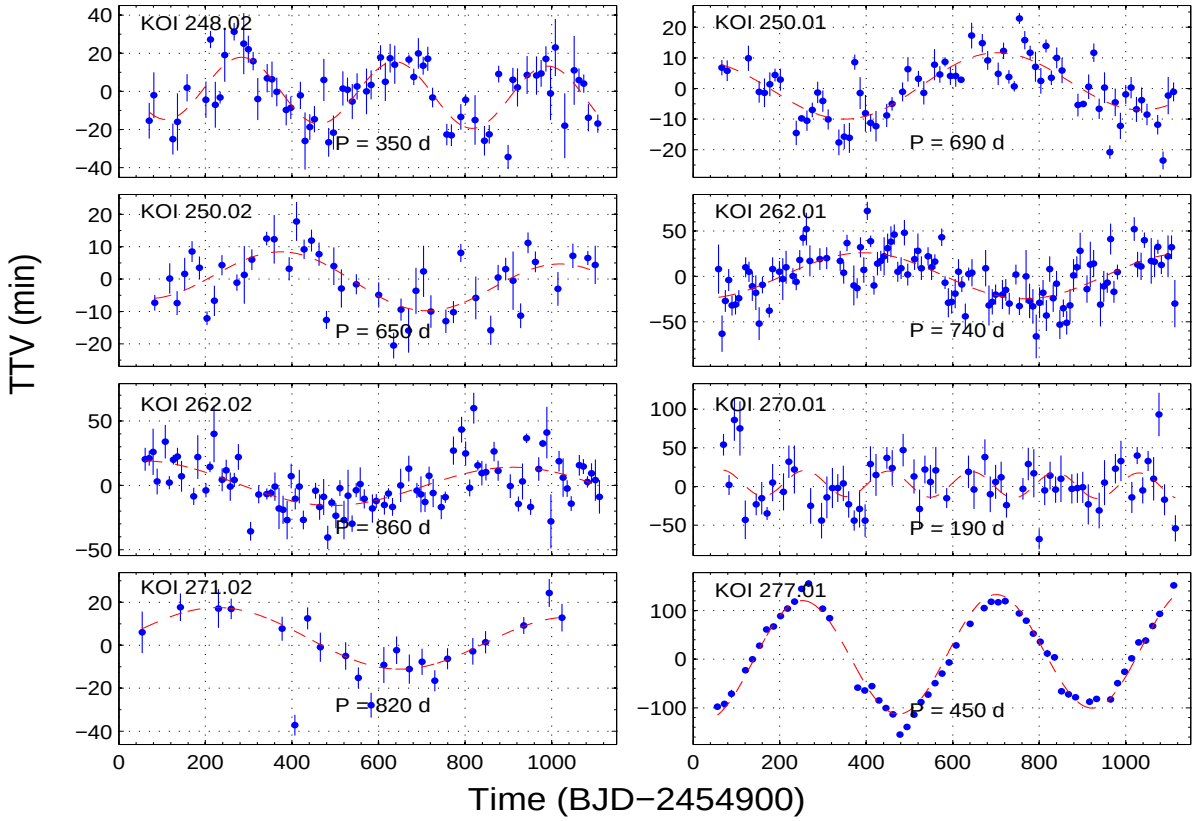

Fig. 4.— KOIs with significant TTVs. See Figure 2 for details.

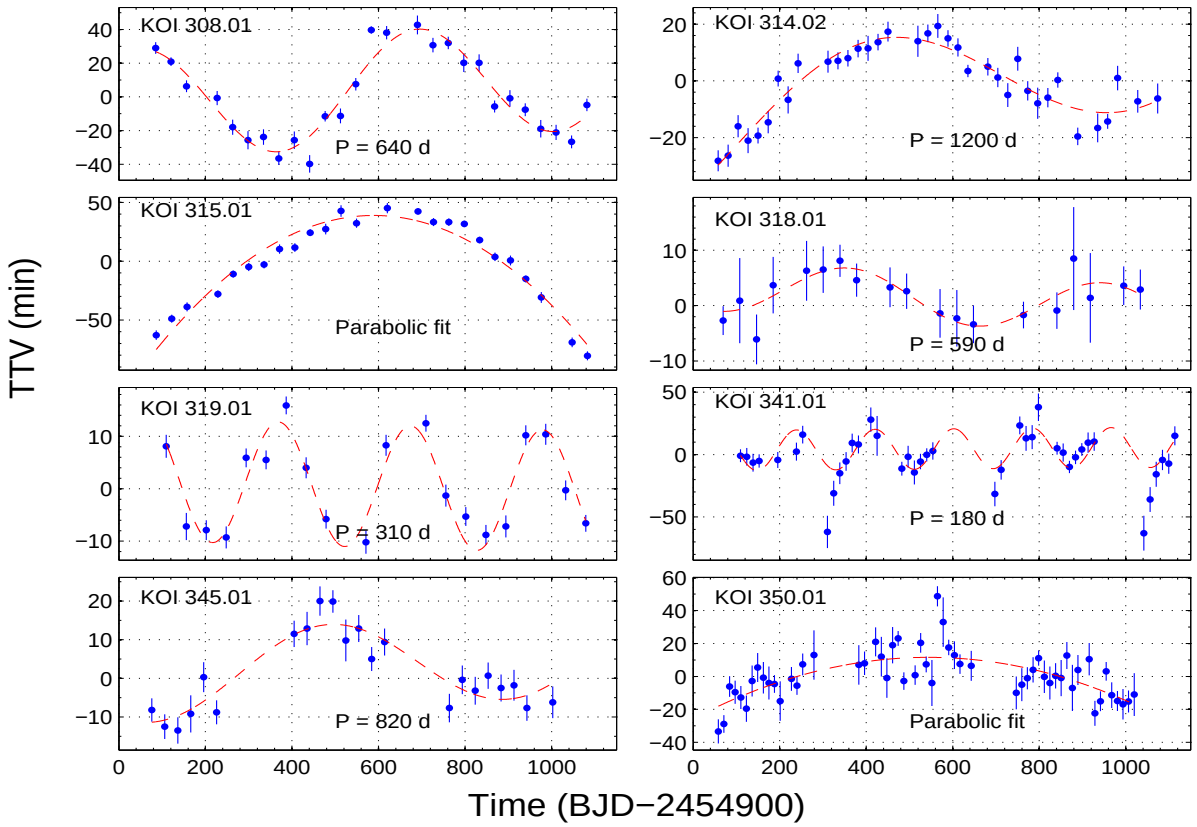

Fig. 5.— KOIs with significant TTVs. See Figure 2 for details.

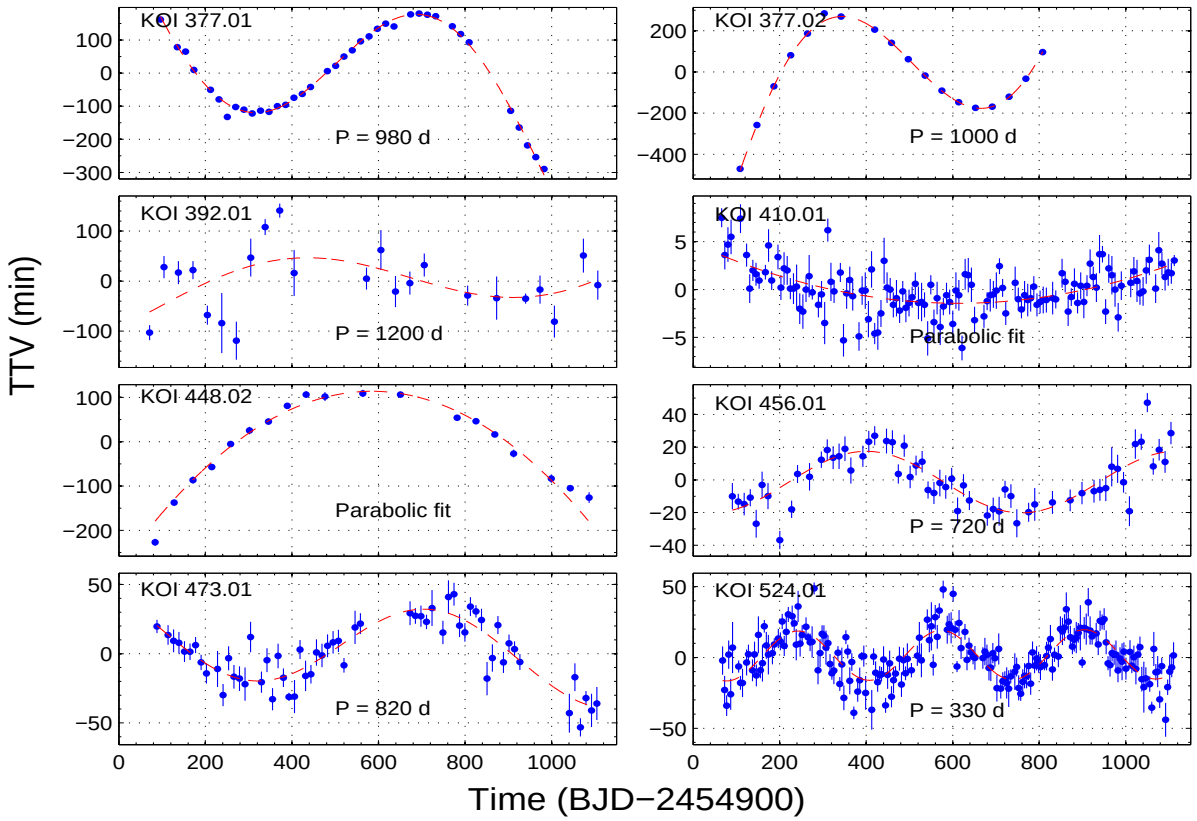

Fig. 6.— KOIs with significant TTVs. See Figure 2 for details.

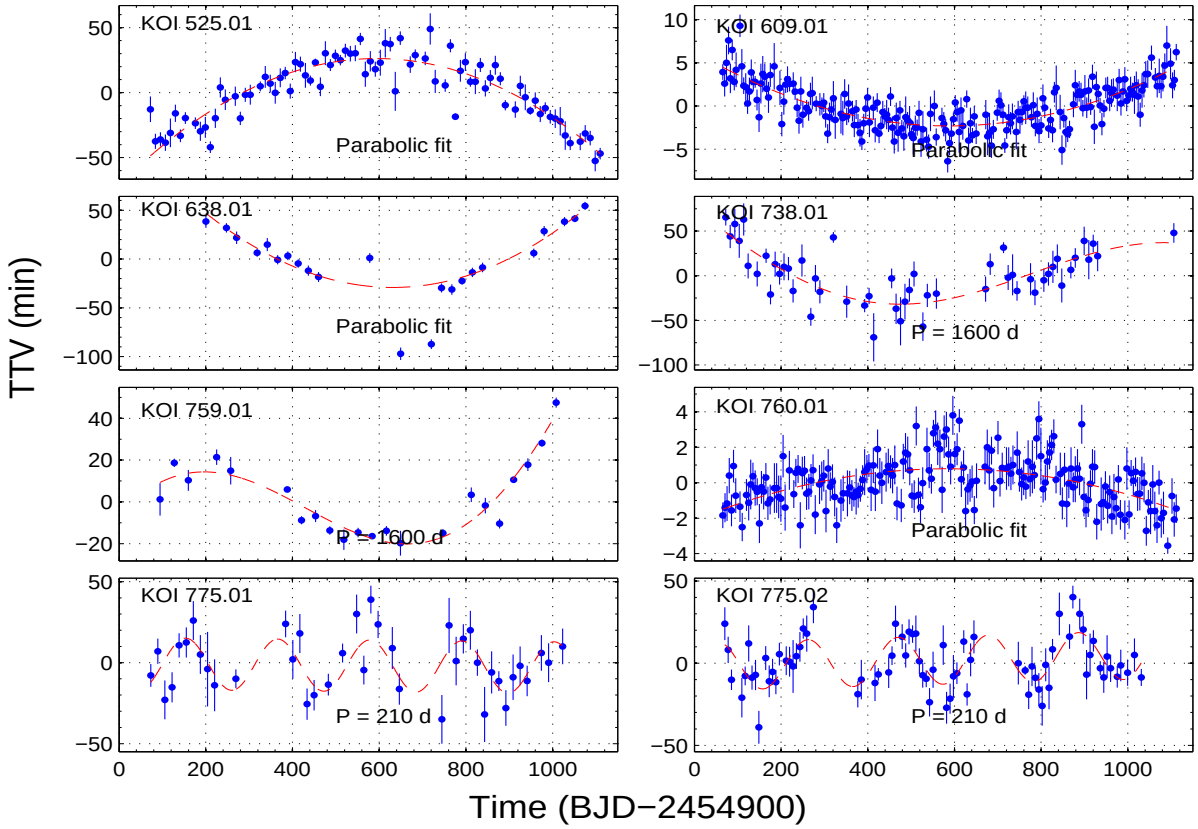

Fig. 7.— The KOIs with significant TTVs. See Figure 2 for details.

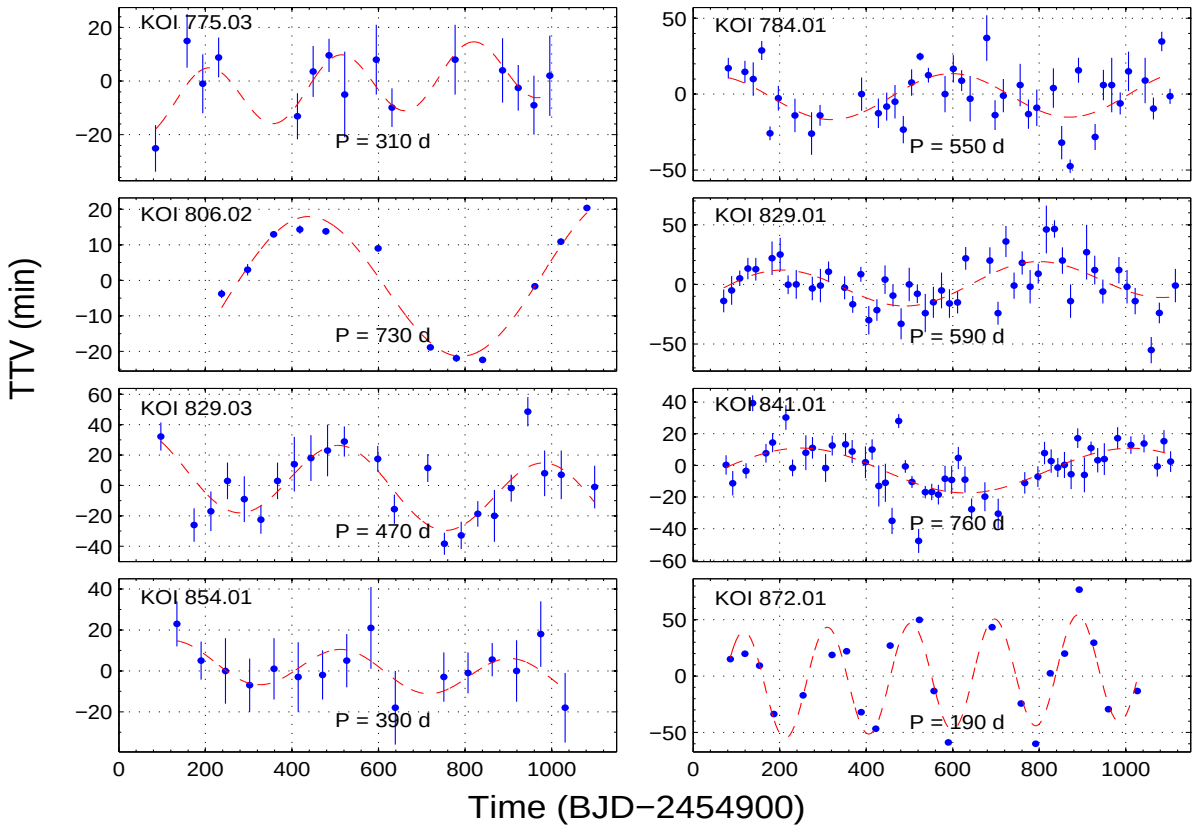

Fig. 8.— The KOIs with significant TTVs. See Figure 2 for details.

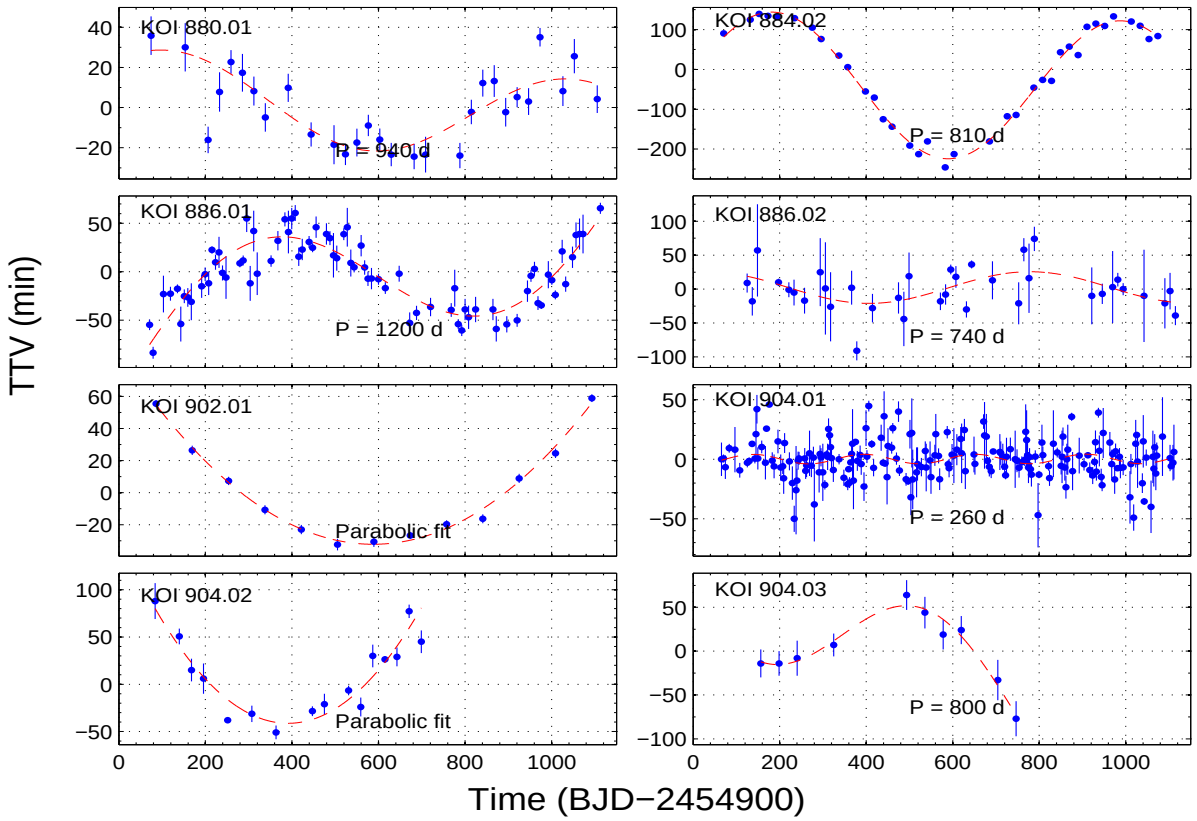

Fig. 9.— The KOIs with significant TTVs. See Figure 2 for details.

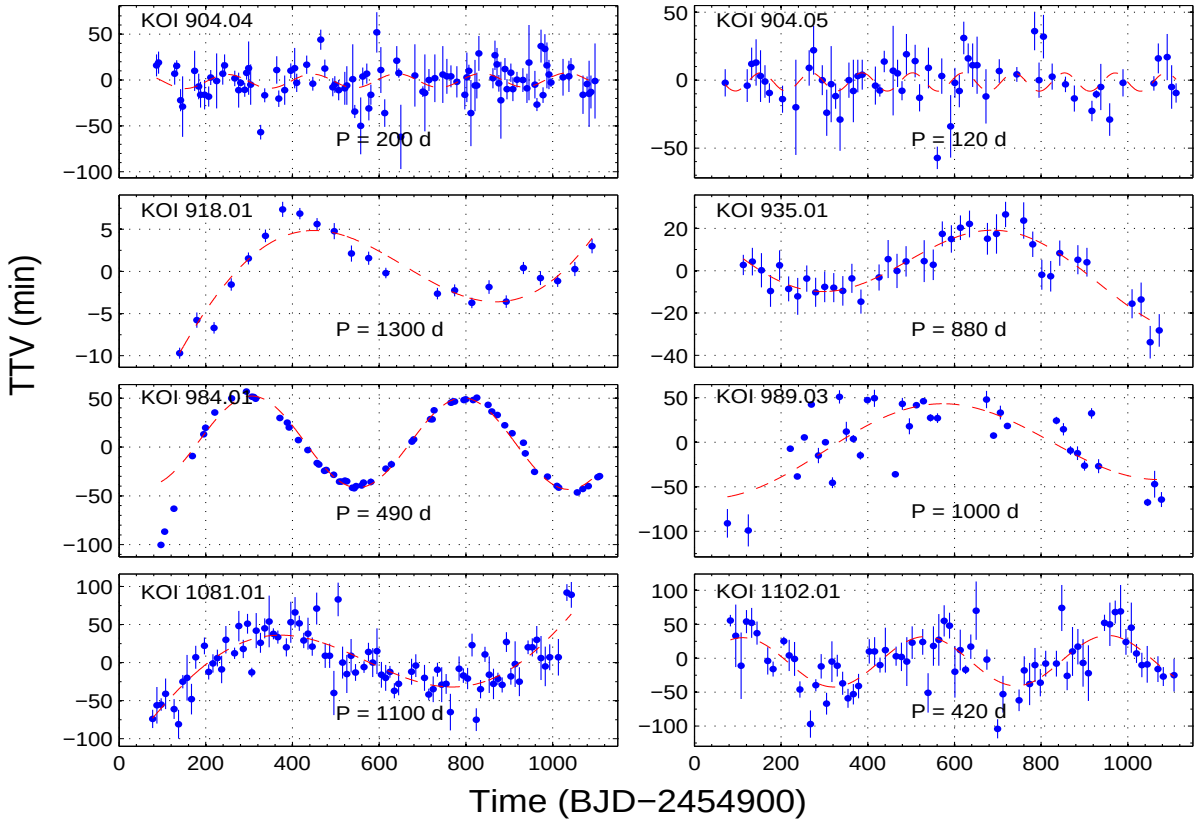

Fig. 10.— The KOIs with significant TTVs. See Figure 2 for details.

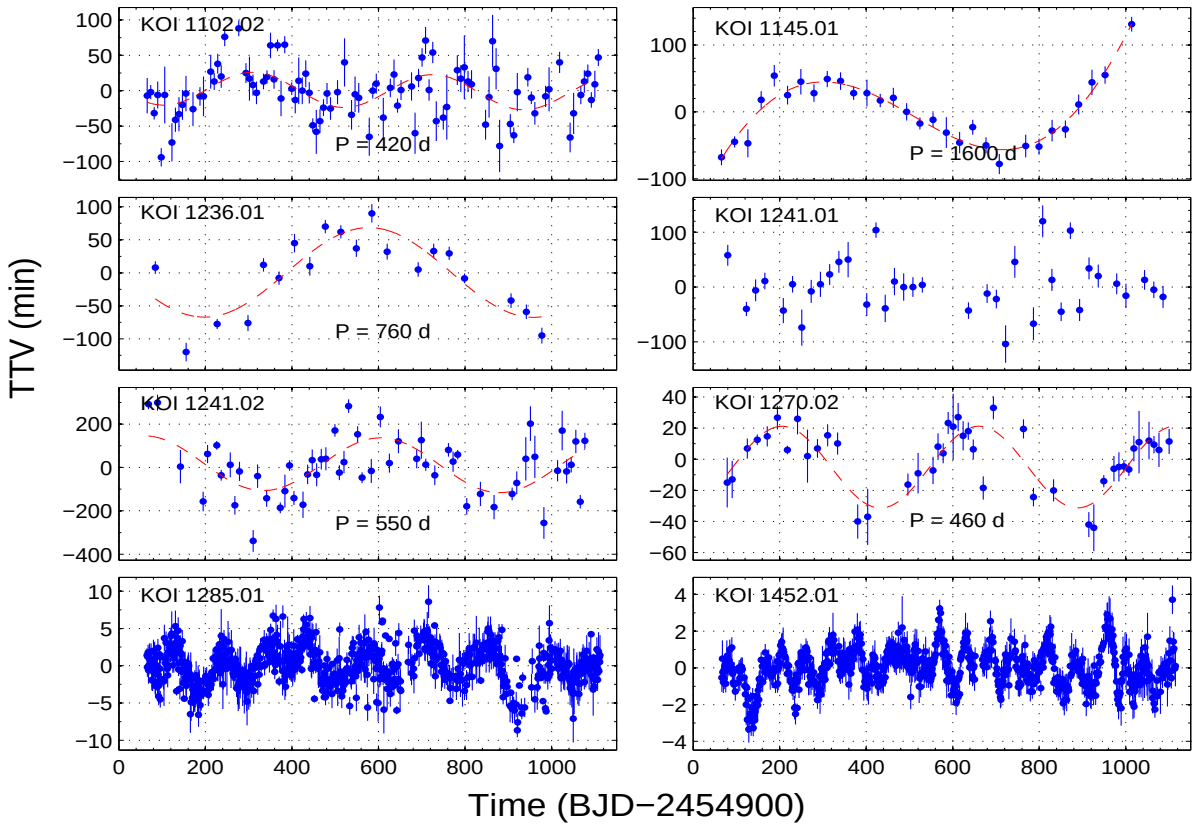

Fig. 11.— The KOIs with significant TTVs. See Figure 2 for details.

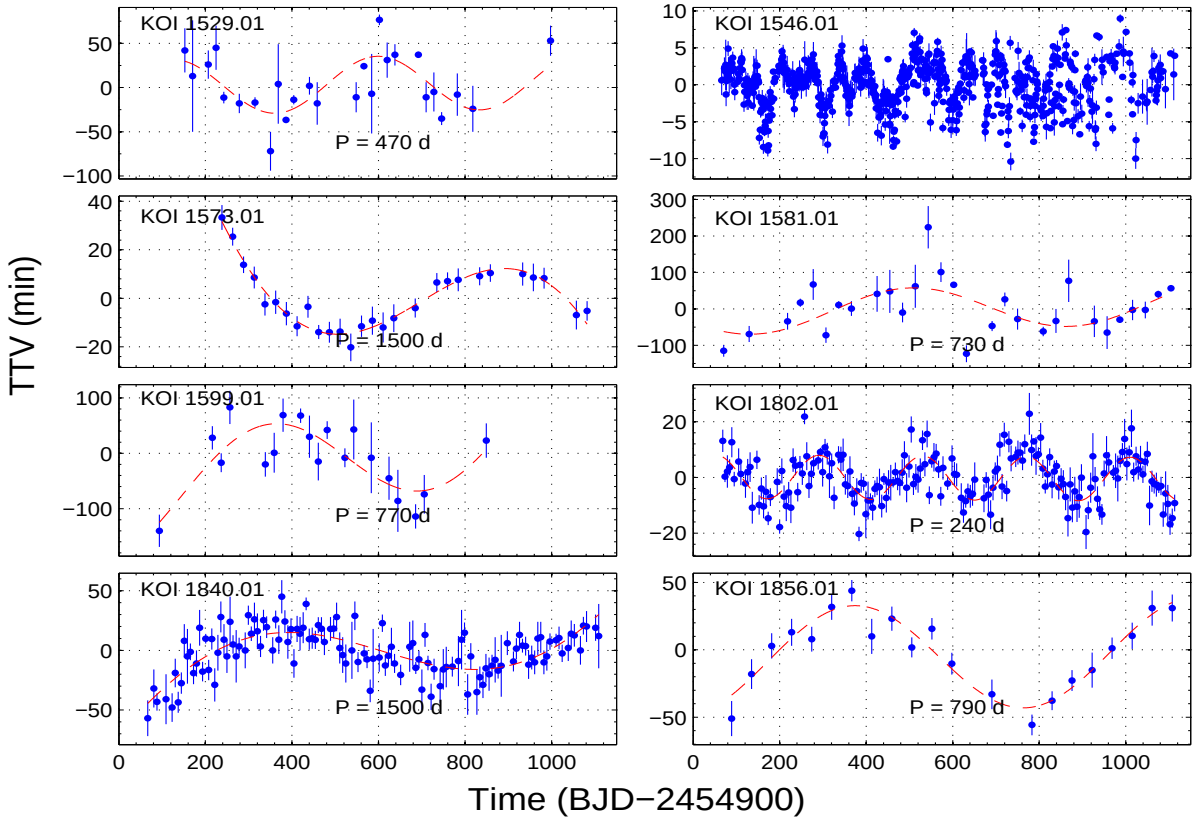

Fig. 12.— The KOIs with significant TTVs. See Figure 2 for details.

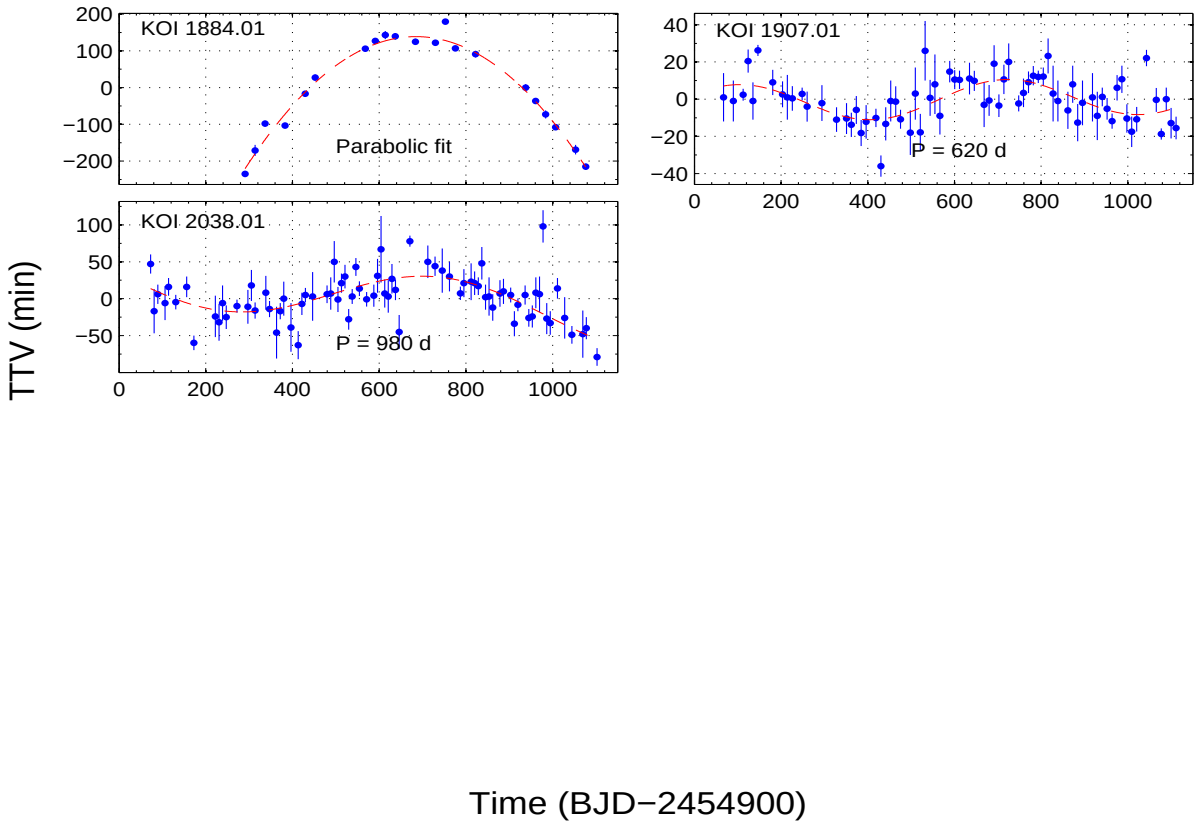

Fig. 13.— The KOIs with significant TTVs. See Figure 2 for details.

5. KOIs with short-period TTV

Our LS analysis of the transiting KOIs yields also 9 systems with highly significant short-period TTV in the range of 3 to 45 days. The modulation amplitudes are relatively small, in the range of 0.3 to 22 min, and it can be detected only because of the periodicity of the modulations and the long time span of the data. Figures 14–16 show the LS periodograms and the folded TTVs of the 9 systems, where one can see the prominent peaks of the periodograms. Table 5 lists the periods and amplitudes found. The table includes references to Section 6, where we briefly comment on these systems.

As pointed out by Szabó et al. (2012b, hereafter Sz12), not all detected short-period modulations are due to physical TTVs. *Apparent* TTV periodicity can be induced either by the long cadence sampling of *Kepler*, or by interference with stellar periodic activity.

The finite sampling rate of the observations can cause a shift of the orbital phases of the observations during a transit, inducing an apparent shift of the derived timing of that transit. This can evoke periodic TTV, with a period of

$$P_{induced} = \frac{P_{orb}}{\frac{P_{orb}}{P_{samp}} - \lfloor \frac{P_{orb}}{P_{samp}} \rfloor} \ , \tag{3}$$

where P_{orb} is the orbital period, P_{samp} is the sampling cadence and $\lfloor x \rfloor$ is the floor of x (Sz12). Note that the induced periodicity is observed with "sampling" intervals equal to the planetary orbit, and therefore the Nyquist frequency of the observations is $1/2P_{orb}$. If the frequency of $P_{induced}$ is larger, we would detect one of its aliases. We found two cases which suggest that the TTV included such effect (see below).

The other effect is due to the stellar spot activity which modulates the stellar intensity with the stellar rotational period. Spot crossing (e.g., Sanchis-Ojeda et al. 2012) during a transit, or a different slope of the stellar brightness during a transit, can cause a shift in the

derived transit timing, inducing an apparent TTV periodicity with the stellar rotational period. In fact, all 9 systems show high level of stellar activity, and we had to check whether the detected TTV periodicity is due to that activity.

To find the frequency of the presumed sampling-induced periodicity, we used for each KOI its P_{orb} from Table 1, and the pertinent P_{samp}, which was ~ 29.424 min for the long cadence, taken to be the median of the differences of the observed timings of that KOI. We also searched for stellar spot periodicity (e.g., McQuillan, Aigrain & Mazeh 2012), and, if presented, checked if its frequency, or one of its aliases, was equal to the TTV one. We plotted the pertinent frequencies in Figures 14–16.

Table 5: KOIs with significant short period TTVs

KOI	Period [d]	Period [d]	σ_P [d]	Amp [min]	σ_A [min]	N	Multi-plicity	Ref.
*258.01	4.16	36.01	0.45	7	1.1	175	1	
*312.01	11.58	39.9	0.48	22.7	1.9	67	2	
*725.01	7.30	22.07	0.12	5.67	0.34	129	1	
*882.01	1.96	45.05	0.61	0.326	0.075	466	1	[1]
*883.01	2.69	9.06	0.045	0.451	0.046	348	1	[1]
*895.01	4.41	32.72	0.37	0.74	0.12	203	1	[1]
*1128.01	0.97	3.36	0.0023	2.91	0.52	544	1	
*1152.01	4.72	11.88	0.042	0.533	0.06	155	1	[1]
*1382.01	4.20	34.38	0.6	1.109	0.081	194	1	[1]

[1] Sz12

*Discussed in Section 6

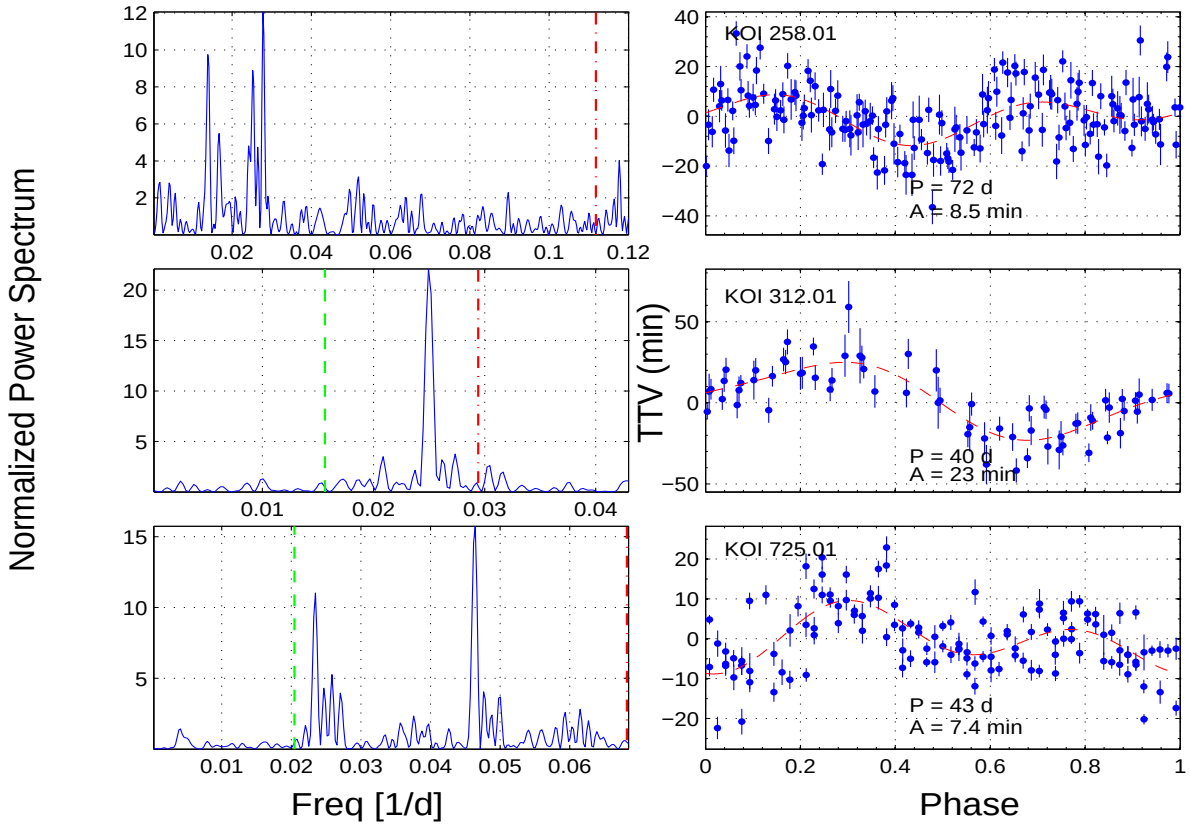

Fig. 14.— The KOIs with short-period TTVs. For each KOI, the LS periodogram and the folded TTV are plotted. The dashed green line represents the stellar activity frequency or one of its aliases, if presented in the stellar light curve, and the dash-dotted red line represents the frequency induced by the sampling.

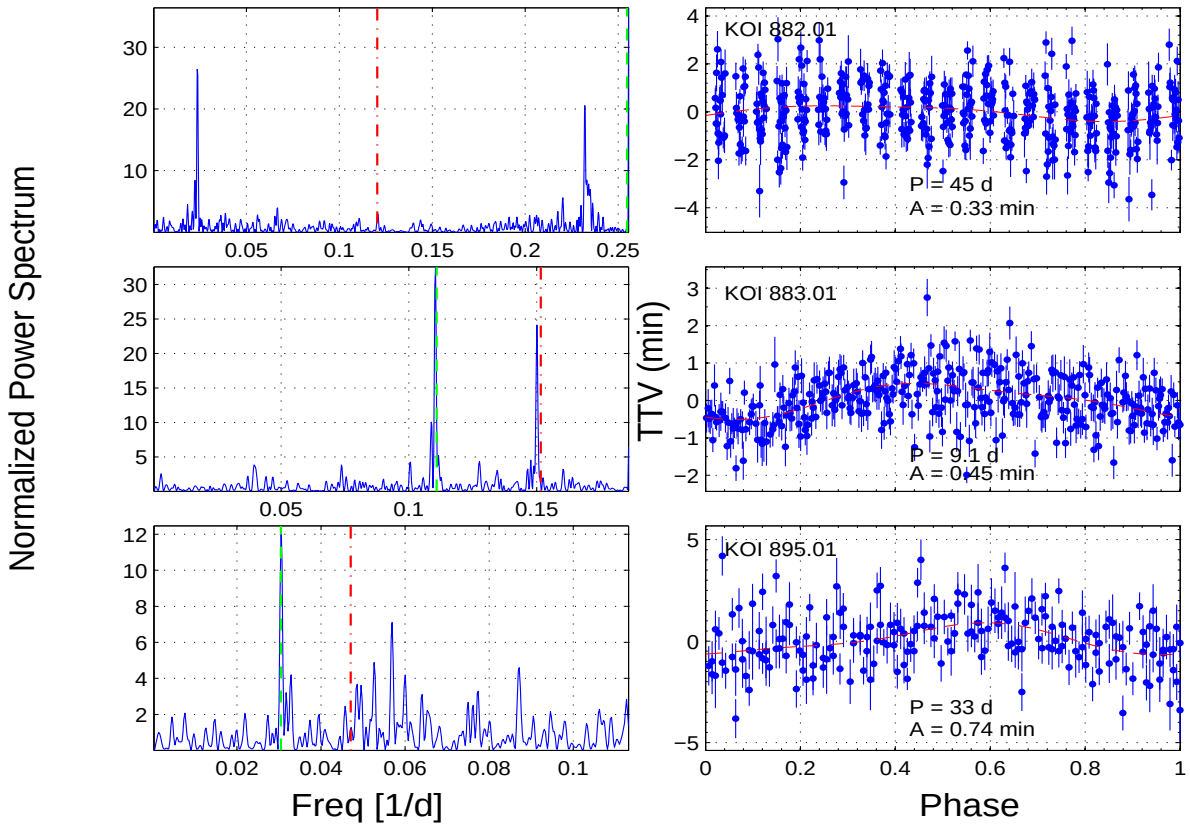

Fig. 15.— The KOIs with short-period TTVs. For each KOI, the LS periodogram and the folded TTV are plotted (see Figure 14 for details).

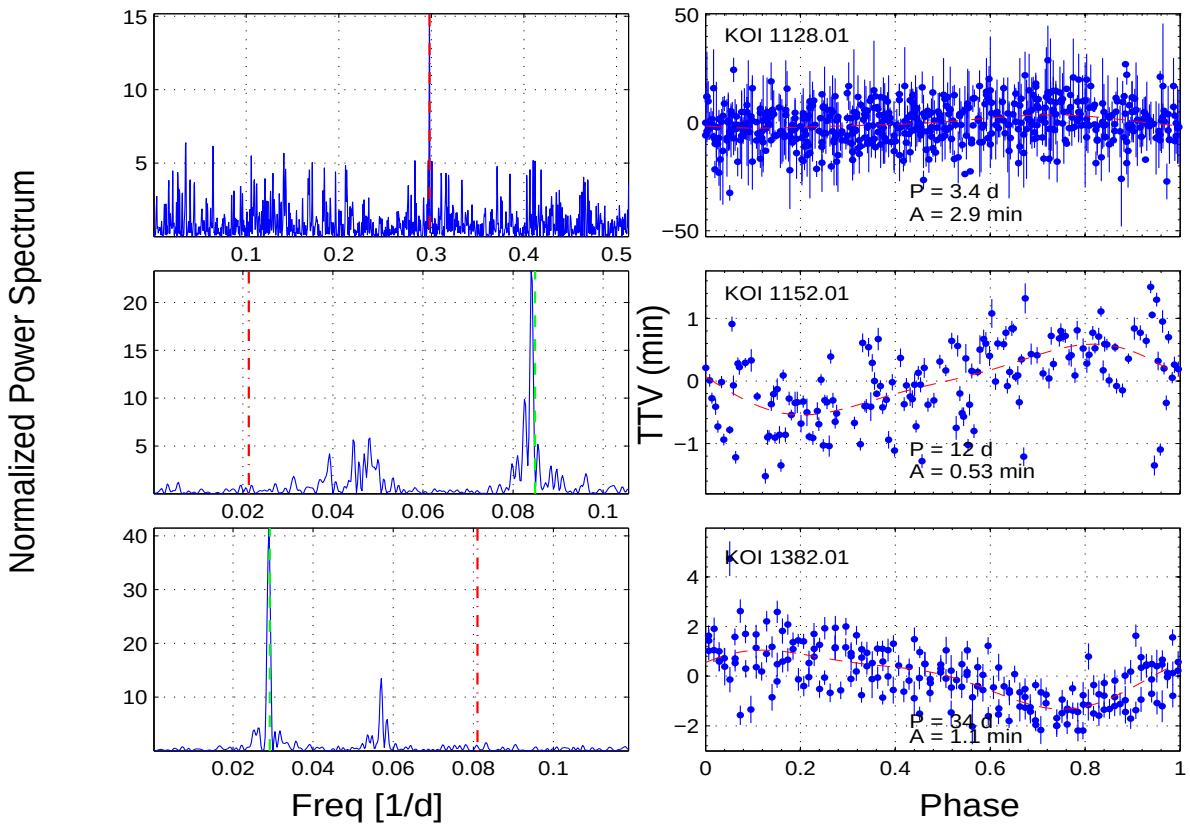

Fig. 16.— The KOIs with short-period TTVs. For each KOI, the LS periodogram and the folded TTV are plotted (see Figure 14 for details).

6. Comments on Individual Systems

In this section we comment on a few KOIs from Tables 4–5. In particular, we folded the light curves of all 100 systems with their orbital period, and looked for a secondary eclipse. For eleven systems we find significant secondary dip, in most cases at phase ~ 0.5, which we interpret as either an eclipse of a secondary star, or as a planetary occultation. In one case we believe that the published period is twice the correct one. We also point out when we suspect that the periodic TTV could be induced either by the long cadence sampling or by the stellar spot periodic activity. Some of these systems were analyzed in a similar way by Sz12, who used six quarters of *Kepler* data to look for TTV periodicity.

- KOI-142.01 (Figure 2): The TTV modulation, with one of the largest amplitudes, could not be fitted with one cosine function. The TTV includes at least two different frequencies, as can be seen in its figure. This could be induced by two additional planets.

- KOI-190.01 (Figure 3): Santerne et al. (2012) found this system to be a diluted eclipsing binary.

- KOI-258.01 (Figure 14): The folded light curve reveals a dip at phase ~ 0.5, probably a secondary eclipse, and therefore the system is probably an eclipsing binary (=EB). The star has significantly high level of activity, probably due to stellar pulsations. The TTV LS periodogram displays two prominent peaks, one is the first harmonic of the other.

- KOI-312.01 (Figure 14): The autocorrelation of the stellar photometry reveals a weak but stable modulation with a short period of 0.17073 d. The green line in the figure is an alias of this frequency.

- KOI-341.01 (Figure 5): The orbital period is probably half the one published and used here.

- KOI-609.01 (Figure 7): Santerne et al. (2012) found this system to be a diluted eclipsing binary. The folded light curve reveals a dip at phase ~ 0.5.

- KOI-725.01 (Figure 14): The folded light curve displays a shallow occultation. The stellar photometry shows a pulsation of 8.58 d. The TTV LS periodogram displays two prominent peaks, one is the first harmonic of the other.

- KOI-882.01 (Figure 15): The photometry displays strong stellar pulsations with a frequency of 3.921 d, very close to twice the orbital period. The second peak in the periodogram is an alias of the first one, relative to the pulsation Nyquist frequency. Sz12 found the same TTV periodicity, with noisier periodogram.

- KOI-883.01 (Figure 15): The TTV LS periodogram displays two prominent peaks. The higher one coincides with the stellar rotation, with a period of 9.02 d, and the smaller one with the induced sampling frequency. Sz12 reached the same conclusion.

- KOI-895.01 (Figure 15): The folded light curve displays a shallow occultation. The star has very pronounced activity, with a period of 5.0935 d, probably due to stellar spots. The TTV LS periodogram displays one prominent peak, with frequency that coincides with the beat frequency with the stellar one. Sz12 identified a different TTV period, close to the third harmonic of the frequency we find.

- KOI-935.01 (Figure 10): The folded light curve probably displays an occultation.

- KOI-984.01 (Figure 10): TTV deviates from the strictly cosine function at $BJD \sim 2454900 + 100$.

- KOI-1128.01 (Figure 16): The TTV LS periodogram displays one prominent peak, with frequency that coincides with the induced sampling one.

- KOI-1152.01 (Figure 16): The TTV LS periodogram displays one prominent peak, with frequency very close to the stellar rotational one, at a period of 2.95 d. Sz12 found a TTV period which is twice the period we found, and did not associated it with the stellar modulation. They also detected a secondary eclipse not in phase 0.5, and concluded that the system is eccentric EB.

- KOI-1241.01 (Figure 11): This planet is part of a known multiple system. KOI-1241.02 shows a clear periodic TTV, and KOI-1241.01 might have anti correlated TTV, as expected. However, the significance of the periodicity of 1241.01 is not high enough to be included in Table 4.

- KOI-1285.01 (Figure 11): The folded light curve, with the orbital period of 0.9374 d, reveals a dip at phase ~ 0.5, probably a secondary eclipse, and therefore the system is probably an EB. The TTVs display coherent modulations, but not a clear stable periodicity. The star has a significant high level of periodic activity, with a period of 0.9362 d, which is close but not identical to the orbital period. Sz12 identified a few different possible TTV periods. They suspected that two of their periods are affected by the stellar modulation.

- KOI-1382.01 (Figure 16): The folded light curve reveals a dip at phase ~ 0.5, probably a secondary eclipse, and therefore the system is probably an EB. The TTV LS periodogram displays one prominent peak, with a frequency that coincides with one of the aliases of the stellar rotational one, at a period of 4.79 d. Sz12 identified the same TTV period, although with much higher first harmonic. They failed to notice that the TTV periodicity comes from the stellar rotation.

- KOI-1452.01 (Figure 11): The folded light curve, with the orbital period of 1.1522 d, reveals a dip at phase ~ 0.5, probably a secondary eclipse, and therefore the system is probably an EB. The TTVs display coherent modulations, but not a clear stable periodicity. The stellar photometry displays strong stellar pulsations with frequencies of 0.65597, 0.7097 and 0.83 d^{-1}. Sz12 found it to be a multi-periodic candidate.

- KOI-1546.01 (Figure 12): The folded light curve, with the orbital period of 0.9176 d, reveals a dip at phase ~ 0.5, probably a secondary eclipse, and therefore the system is probably an EB. The TTVs display coherent modulations until $BJD \sim 2454900+600$, but not a clear stable periodicity. The stellar photometry displays a strong periodicity of 0.933 d, probably due to stellar rotation, a period very close but not identical to the orbital period. Sz12 found it to be a multi-periodic candidate.

7. Discussion

We presented here 100 KOIs with highly significant TTVs, 91 with long-term modulations (Section 4, Table 4), and nine KOIs with short-period low-amplitude TTV periodicities (Section 5, Table 5). Out of the 91 systems, 76 showed clear periodicities, with well determined periods and amplitudes. Another 11 KOIs had periods too long to be established without a doubt. For those we need to wait for more data before the TTV period can be safely determined. Another four systems display coherent modulations, but not a clear stable periodicity.

As discussed in Section 6, some TTVs, the nine short-period ones in particular, can be due to some interference with stellar photometric modulation, or some other "instrumental" effect. However, let us assume that most of the observed *long-term* periodic TTVs of the Kepler KOIs are caused by dynamical interaction between planets, as predicted by

Agol et al. (2005) and Holman & Murray (2005). For the single-planet KOIs, let us further assume that the interaction is induced by an unseen additional planet. We did not detect the transits of the additional planet either because of a larger inclination angle relative to our line of sight, or because its radius was too small. We presented here 37 single-KOI planets with significant TTVs, 7 of which were with TTV periodicity probably longer than $\sim$ 2000 days. On the other hand, only 4 out of 54 multiple KOIs with significant TTVs showed an indication for long-term periodicity.

The different fraction of KOIs with long-term modulations among the single and multiple KOIs, *if real*, is intriguing. The longer TTV period could be due to the fact that the additional unseen planet is closer to a mean-motion resonance. If this is true, we can conjecture that pairs of planets with orbital periods close to a resonance tend to have larger relative inclinations. Another possibility is that we did not detect the additional planets in the single-KOI systems because the other planet is either too small or has a large orbit. Both features are expected to produce longer TTV periodicities.

We also find an indication for some correlation between the KOI period and the period of its TTV, as can be seen in Figure 17. This is of no surprise, as the orbital period of a planet is the natural time unit of the dynamical interaction, and therefore we expect the TTV periodicity to be correlated with this time unit. Another correlation, between the amplitudes and the periods of the detected TTV periodicities, emerges from the present sample (see Figure 18), as was predicted, for example, by Agol et al. (2005). The same correlation appears when we plot the amplitude in units of the KOI orbital period.

We pointed out possible non-physical origin of some of the TTVs presented here. In particular, the short-period modulations could be due to either to the long cadence sampling of *Kepler* or by stellar spot periodic activity (Sz12). We found evidence that 4 out of the 9 short-period detected TTVs are due to the stellar periodicity. We also found that

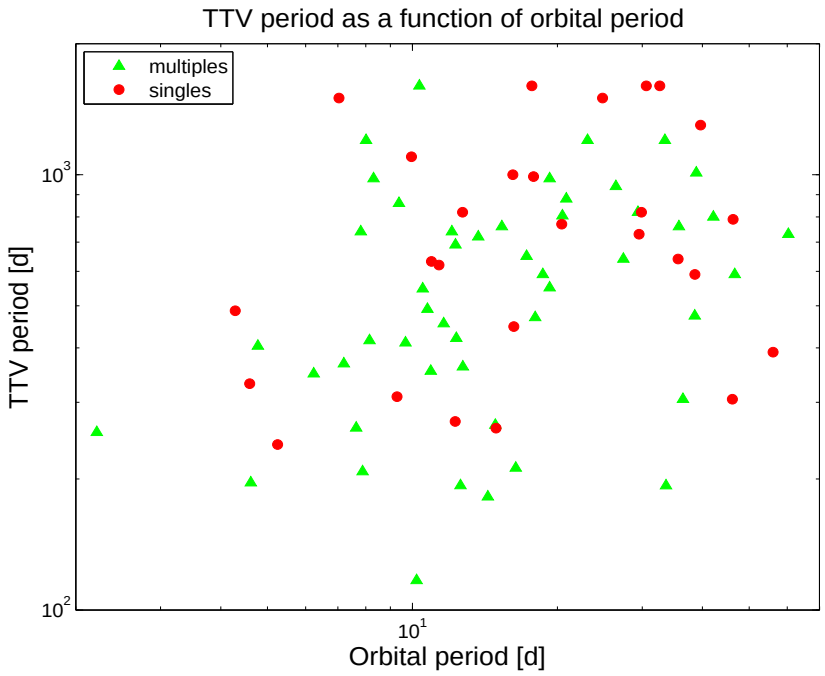

Fig. 17.— The TTV period as a function of the orbital period. Plot is on a log-log scale. Single KOIs are plotted with red circles, and multiples with green triangles.

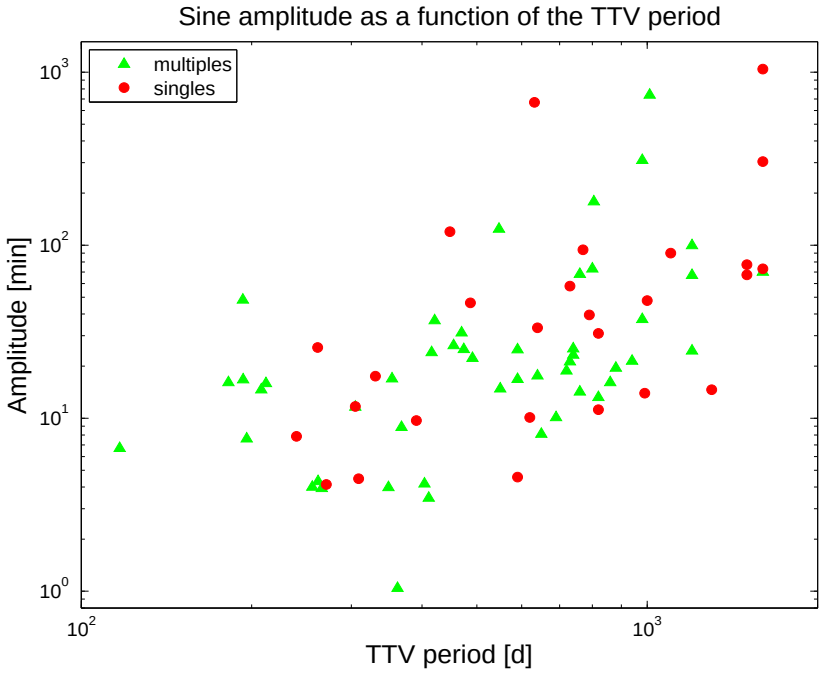

Fig. 18.— The amplitude of the TTV modulation as a function of its period. Plot is on a log-log scale. Single KOIs are plotted with red circles, and multiples with green triangles.

KOI-883.01 and 1128.01 show a periodicity induced by the Kepler sampling.

The sample of 100 KOIs with significant TTVs includes 54 systems discussed by F11 (16 KOIs), F12 (36 KOIs) and S12 (18 KOIs), all based only on a fraction of the data available now. References to those three works can be found in Table 4. It is interesting to compare the analysis of F11, F12 and S12 on one hand and the present results on the other hand, and see how doubling the time span can change our assessment of the nature of the modulation. In many cases the time span of the first 6 quarters was not long enough to detect a local maximum *and* minimum of the TTV modulation, and therefore the periodicity of the modulation could not be estimated. One illustrious example is KOI-142, with its peak-to-peak amplitude of more than 1200 min.

One could hope that the accumulating details of the observed TTV could give some hints for the orbital elements of the perturbing unseen planet, at least for some of the single KOIs. However, as discussed already by Holman & Murray (2005) and Agol et al. (2005), the amplitude and periodicity of the TTV modulation depends on various parameters, in particular the mass and orbital period of the unseen planet and how close the orbits of the two planets are to some mean motion resonance. Therefore, it is quite difficult to deduce the parameters of the unseen planet, although some stringent constraints can be derived, as was done by Ballard et al. (2011) for Kepler-19. We hope that the available catalog will push towards similar work on other single-KOI systems with significant TTV.

One parameter that bears interesting implications on our understanding of the planetary formation is the relative inclination between the plane of motion of the observed planet and that of the presumed interacting planet for the single KOI with significant TTV. Relative inclination can induce a precession of the orbital motion of the observed planet, which can manifest itself in a modulation of the transit duration and depth (TDV and TPV). Although the focus of the present work is on the TTVs, the catalog, which includes

derived TDV and TPV, can, in principle, help to point out systems with relative inclination. Furthermore, stringent upper limit on TDV and TPV for systems with detected TTVs can help to constrain the relative inclination between the planets.

However, an observed precession is not necessarily induced by a planet with a non-vanishing relative inclination. An observed precession just proves that the total angular momentum of the system is not parallel to the orbital angular momentum of the transiting planet. The origin of the precession could be misalignment of the stellar rotation axis relative to the angular momentum of the planet, an idea that was unthinkable not long ago, but has now solid evidence in the accumulating data (see Winn 2011). An example for this idea is KOI-13 (Szabó et al. 2011, see also Figure 1). Regardless, we suggest that systems with detected significant TDV and TPV deserve further close study.

Finally, we present here a systematic TTV analysis of twelve quarters of *Kepler* observations of all KOIs. One could expect that the derived TTVs, for the single KOIs in particular, could help constructing a *statistical* picture of the frequency and architecture of the population of the planetary multiple systems of the Kepler KOIs (e.g., Ford et al. 2011, 2012), like the discussion that followed the discoveries of *Kepler* multiple transiting planets (e.g., Lissauer et al. 2011b; Steffen et al. 2010). To perform such a statistical analysis one needs to model the dependence of the detectability of TTV coherent modulation on the parameters of the unseen perturbing planet, and to convolve it with the observed parameters of the transit, like its SNR and duration, together with the orbital period of the transiting planet. The present catalog can be used for such a study.

The research leading to these results has received funding from the European Research Council under the EU's Seventh Framework Programme (FP7/(2007-2013)/ ERC Grant Agreement No. 291352). All photometric data presented in this paper were obtained from the Mikulsky Archive for Space Telescopes (MAST). STScI is operated by the Association of

Universities for Research in Astronomy, Inc., under NASA contract NAS5-26555. Support for MAST for non-HST data is provided by the NASA Office of Space Science via grant NNX09AF08G and by other grants and contracts.

REFERENCES

Agol, E., Steffen, J., Sari, R., & Clarkson, W. 2005, MNRAS, 359, 567

Batalha, N. M., Rowe, J. F., Bryson, S. T., et al. 2012, arXiv:1202.5852

Ballard, S., Fabrycky, D., Fressin, F., et al. 2011, ApJ, 743, 200

Borucki, W. J., Koch, D. G., Basri, G., et al. 2011, ApJ, 736, 19

Carter, J. A., Agol, E., Chaplin, W. J., et al. 2012, Science, 337, 556

Cochran, W. D., Fabrycky, D. C., Torres, G., et al. 2011, ApJS, 197, 7

Fabrycky, D. C., Ford, E. B., Steffen, J. H., et al. 2012, ApJ, 750, 114

Ford, E. B., Rowe, J. F., Fabrycky, D. C., et al. 2011, ApJS, 197, 2

Ford, E. B., Fabrycky, D. C., Steffen, J. H., et al. 2012, ApJ, 750, 113

Ford, E. B., Ragozzine, D., Rowe, J. F., et al. 2012, ApJ, 756, 185

Holman, M. J., & Murray, N. W. 2005, Science, 307, 1288

Holman, M. J., Fabrycky, D. C., Ragozzine, D., et al. 2010, Science, 330, 51

Lissauer, J. J., Fabrycky, D. C., Ford, E. B., et al. 2011a, Nature, 470, 53

Lissauer, J. J., Ragozzine, D., Fabrycky, D. C., et al. 2011b, ApJS, 197, 8

McQuillan, A., Aigrain, S., & Mazeh, T. 2012, submitted to MNRAS

Mandel, K., & Agol, E. 2002, ApJ, 580, L171

Mazeh, T., Nachmani, G., Sokol, G., Faigler, S., & Zucker, S. 2012, A&A, 541, A56

Nesvorny, D., Kipping, D. M., Buchhave, L. A., et al. 2012, Science, 336, 1133

Sanchis-Ojeda, R., Fabrycky, D. C., Winn, J. N., et al. 2012, Nature, 487, 449

Santerne, A., Díaz, R. F., Moutou, C., et al. 2012, A&A, 545, A76

Steffen, J. H., Batalha, N. M., Borucki, W. J., et al. 2010, ApJ, 725, 1226

Steffen, J. H., Ford, E. B., Rowe, J. F., et al. 2012, ApJ, 756, 186

Steffen, J. H., Fabrycky, D. C., Ford, E. B., et al. 2012, MNRAS, 421, 2342

Steffen, J. H., Fabrycky, D. C., Agol, E., et al. 2013, MNRAS, 428, 1077

Szabó, G. M., Szabó, R., Benkő, J. M., et al. 2011, ApJ, 736, L4

Szabó, G. M., Pál, A., Derekas, A., et al. 2012, MNRAS, 421, L122

Szabó, R., Szabó, G. M., & Dálya, G. 2012, arXiv:1207.7229

Tamuz, O., Mazeh, T., & North, P. 2006, MNRAS, 367, 1521

Tingley, B., Palle, E., Parviainen, H., et al. 2011, A&A, 536, L9

Wang, S., Ji, J., & Zhou, J.-L. 2012, ApJ, 753, 170

Winn, J. N. 2011, European Physical Journal Web of Conferences, 11, 5002